



ORIGINAL ARTICLE

Design, synthesis and biological evaluation of isoxazole-naphthalene derivatives as anti-tubulin agents



Guangcheng Wang^{a,b,*}, Wenjing Liu^{a,c,e}, Yong Huang^a, Yongjun Li^c,
Zhiyun Peng^{d,*}

^a State Key Laboratory of Functions and Applications of Medicinal Plants, Guizhou Provincial Key Laboratory of Pharmaceutics, Guizhou Medical University, Guiyang, China

^b College of Chemistry and Chemical Engineering, Jishou University, Jishou, China

^c Engineering Research Center for the Development and Application of Ethnic Medicine and TCM (Ministry of Education), Guizhou Medical University, Guiyang, China

^d College of Food Science and Technology, Shanghai Ocean University, Shanghai, China

^e School of Pharmacy, Guizhou Medical University, Guiyang, China

Received 10 March 2020; accepted 12 April 2020

Available online 18 April 2020

KEYWORDS

Isoxazole;
Naphthalene;
Anti-tubulin agents;
Tubulin polymerization;
Antitumor

Abstract In this study, a novel series of isoxazole-naphthalene derivatives as tubulin polymerization inhibitors were designed, synthesized and evaluated for their anti-proliferative activities against human breast cancer cell line MCF-7. Most of the synthesized compounds exhibited moderate to potent antiproliferative activity ($IC_{50} < 10.0 \mu M$), as compared to cisplatin ($15.24 \pm 1.27 \mu M$). Among them, compound **5j** containing 4-ethoxy substitution at phenyl ring was found to be the most active compound with IC_{50} value of $1.23 \pm 0.16 \mu M$. Mechanistic studies revealed that compound **5j** arrested cell cycle at G2/M phase and induces apoptosis. Furthermore, *in vitro* tubulin polymerization assay showed that compound **5j** displayed better inhibition activity on tubulin polymerization ($IC_{50} = 3.4 \mu M$) than colchicine ($IC_{50} = 7.5 \mu M$). Molecular docking study also revealed that compound **5j** binds to the colchicine binding site of tubulin.

© 2020 The Author(s). Published by Elsevier B.V. on behalf of King Saud University. This is an open access article under the CC BY-NC-ND license (<http://creativecommons.org/licenses/by-nc-nd/4.0/>).

* Corresponding authors at: State Key Laboratory of Functions and Applications of Medicinal Plants, Guizhou Provincial Key Laboratory of Pharmaceutics, Guizhou Medical University, Guiyang, China (G. Wang); College of Food Science and Technology, Shanghai Ocean University, Shanghai, China (Z. Peng).

E-mail addresses: wanggch123@163.com (G. Wang), pengzhiyun1986@163.com (Z. Peng).

Peer review under responsibility of King Saud University.



1. Introduction

Microtubules are the major dynamic structural components of the cytoskeleton in eukaryotic cells, which are composed of α - and β -tubulin heterodimers (Downing and Nogales, 1998a). They play critical roles in a wide range of various cellular processes such as maintenance of cell shape, intracellular vesicle transport, regulation of motility, cell signaling, and cell division and replication (Desai and Mitchison, 1997; Downing and Nogales, 1998b; Wilson et al., 1999; Amos, 2011). Therefore, anti-tubulin agents can disrupt microtubule dynamics resulting in cell cycle arrest in G2/M phase and subsequently leading to tumor cell death by apoptosis (Jordan et al., 1998). Furthermore, all microtubule-binding drugs (both microtubule-stabilizing and microtubule-destabilizing) have antiangiogenic and vascular-disrupting properties through inhibit endothelial cell proliferation, migration, and tube formation (Schwartz, 2009). Because of the important roles of microtubules in cell division and other cellular processes, tubulin have been recognized as an important target for the discovery and development of anticancer drug (Hadfield et al., 2003; Jordan and Wilson, 2004; Zhou and Giannakakou, 2005; Stanton et al., 2011; Kaur et al., 2014). Many antimetabolic agents have been widely used in the clinical for the treatment of different human cancers over the past decade, such as paclitaxel, docetaxel, vinblastine, vincristine, eribulin mesylate, and ixabepilone (Jordan and Wilson, 2004). However, these clinical drugs have some disadvantages including the high toxicity, the development of drug resistance, side effects, poor solubility, low oral bioavailability and complex synthesis (Messaoudi et al., 2009). Hence, discovery and development of new anti-tubulin agents are still urgently needed.

Isoxazole is an important heterocyclic nucleus, which is present in many naturally occurring products and synthetic compounds. In recent years, isoxazole and its derivatives have attracted much attention for chemists and pharmacologists due to their broad spectrum of biological activities (Sysak and Obmińska-Mrukowicz, 2017; Zhu et al., 2018), such as antifungal (Santos et al., 2010), antimicrobial (Badadhe et al., 2013), anti-inflammatory (Gorantla et al., 2017), anti-HIV (Gomha et al., 2014), anti-aging (Koufaki et al., 2014),

neuroprotective (Colleoni et al., 2008), antidiabetic (Zhou et al., 2010), antidepressant (Yu et al., 2012) and anticancer activities (Caliskan et al., 2018). Furthermore, several compounds containing isoxazole moiety have been reported as anticancer agents by inhibiting tubulin polymerization (Fig. 1, I–III) (Simoni et al., 2005; Shin et al., 2008; Wu et al., 2009; Lee et al., 2011). On the other hand, naphthalene is an important pharmacophoric fragment for the design and development of anti-tubulin agents (Medarde et al., 2004). Some of the naphthalene derivatives have been reported as tubulin polymerization inhibitors (Fig. 1, IV–VI) (Maya et al., 2005; Alvarez et al., 2008; Wang, et al., 2018a).

Over the years, molecular hybridization is a powerful strategy in drug design and development (Viegas-Junior et al., 2007). Hence, in continuation of our interest in the design and development of novel tubulin polymerization inhibitors (Wang et al., 2012; Wang et al., 2014; Wang, et al., 2018b), herein we report for the first time the synthesis of isoxazole-naphthalene derivatives by incorporating isoxazole and naphthalene moiety in a single molecule (Fig. 2). All the synthesized compounds were evaluated for their antiproliferative activity against human breast cancer cell line MCF-7. The mechanism of antiproliferative effects of representative compound **5j** was studied by using *in vitro* tubulin polymerization, cell cycle arrest, and cell apoptosis assay. Furthermore, molecular modeling study was performed to elucidate the binding mode of compound **5j** in the colchicine binding site of tubulin.

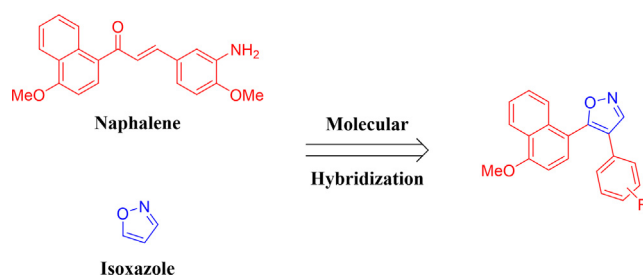


Fig. 2 Rationale design of the title compounds of this study.

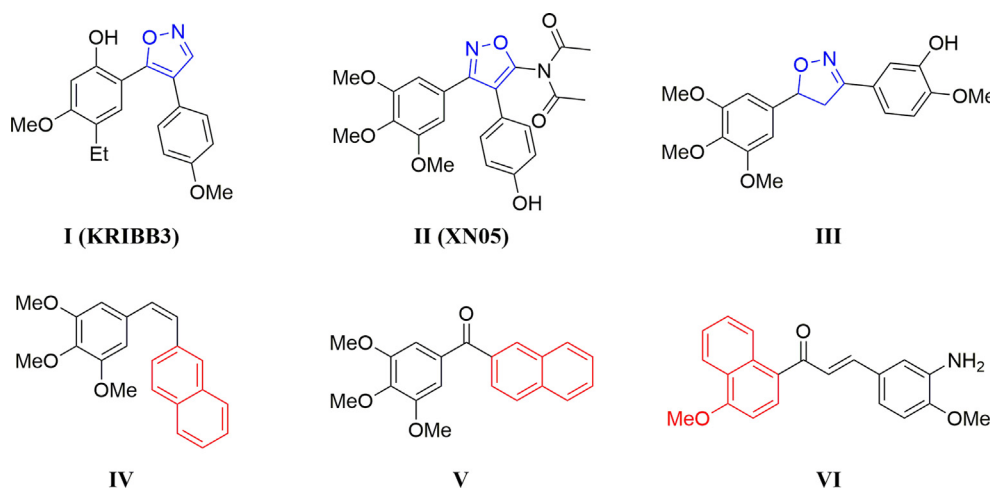


Fig. 1 Chemical structures of some tubulin polymerization inhibitors containing isoxazole or naphthalene ring.

2. Experimental

2.1. Chemistry

All starting materials and reagents were purchased from commercial suppliers. TLC was performed on 0.20 mm Silica Gel 60 F₂₅₄ plates (Qingdao Ocean Chemical Factory, Shandong, China). Nuclear magnetic resonance spectra (NMR) were recorded on a Bruker spectrometer (400 MHz) with TMS as an external reference and reported in parts per million.

2.1.1. General procedure for the synthesis of **5a-5u**

To a solution of compound **4** (0.36 mmol) in 15 ml MeOH/H₂O (2:1) was added Hydroxylamine hydrochloride (0.4 mmol, 27.8 mg) and Na₂CO₃ (0.52 mmol, 55 mg), and the mixture was acidified with acetic acid to pH 4–5. After the mixture was stirred at 70 °C for 24 h. The resulting solution was poured into aqueous NaHCO₃ (50 ml), extracted with ethyl acetate (25 ml × 3). The extract was dried with anhydrous Na₂SO₄ and concentrated under vacuum. The residue was purified by chromatography on silica gel with petroleum ether/ethyl acetate to give the product **5a-5u**.

2.1.1.1. 5-(4-Methoxynaphthalen-1-yl)-4-(3,4,5-trimethoxyphenyl)isoxazole (5a). Yellow solid, yield 74%. ¹H NMR (400 MHz, CDCl₃) δ (ppm): 3.47 (s, 6H), 3.77 (s, 3H), 4.05 (s, 3H), 6.39 (s, 2H), 6.86 (d, 1H, *J* = 8.0 Hz), 7.41–7.46 (m, 1H), 7.47–7.51 (m, 1H), 7.54 (d, 1H, *J* = 8.0 Hz), 7.63 (d, 1H, *J* = 8.4 Hz), 8.31 (d, 1H, *J* = 7.6 Hz), 8.63 (s, 1H); ¹³C NMR (100 MHz, CDCl₃) δ (ppm): 55.9, 55.9, 61.0, 103.3, 104.5, 117.6, 117.8, 122.5, 125.1, 125.3, 125.7, 125.9, 127.8, 129.7, 132.1, 137.4, 150.2, 153.4, 157.5, 164.7; HRMS (ESI) calcd for [M + H]⁺ C₂₃H₂₂NO₅⁺: 392.14925 found 392.14603.

2.1.1.2. 5-(4-Methoxynaphthalen-1-yl)-4-(4-methoxyphenyl)isoxazole (5b). Yellow oil, yield 75%. ¹H NMR (400 MHz, CDCl₃) δ (ppm): 3.71 (s, 3H), 4.02 (s, 3H), 6.71 (d, 2H, *J* = 8.8 Hz), 6.81 (d, 1H, *J* = 8.0 Hz), 7.12 (d, 2H, *J* = 8.8 Hz), 7.41–7.45 (m, 1H), 7.47–7.51 (m, 2H), 7.69 (d, 1H, *J* = 8.8 Hz), 8.33 (d, 1H, *J* = 8.4 Hz), 8.60 (s, 1H); ¹³C NMR (100 MHz, CDCl₃) δ (ppm): 55.3, 55.8, 103.5, 114.3, 117.7, 117.7, 122.1, 122.5, 125.3, 125.8, 125.9, 127.7, 128.6, 129.6, 132.2, 150.6, 157.4, 159.0, 164.2; HRMS (ESI) calcd for [M + H]⁺ C₂₁H₁₈NO₃⁺: 332.12812 found 332.12601.

2.1.1.3. 5-(4-Methoxynaphthalen-1-yl)-4-(*p*-tolyl)isoxazole (5c). Yellow oil, yield 86%. ¹H NMR (400 MHz, CDCl₃) δ (ppm): 2.13 (s, 3H), 3.98 (s, 3H), 6.95 (d, 2H, *J* = 8.0 Hz), 7.01 (dd, 1H, *J* = 8.0 Hz, 1.2 Hz), 7.10 (d, 2H, *J* = 8.0 Hz), 7.40–7.50 (m, 3H), 7.53 (d, 1H, *J* = 8.0 Hz), 8.21 (d, 1H, *J* = 8.4 Hz), 9.12 (s, 1H); ¹³C NMR (100 MHz, CDCl₃) δ (ppm): 21.2, 56.4, 104.7, 117.5, 118.1, 122.7, 125.0, 125.5, 126.5, 126.7, 127.3, 128.3, 129.8, 130.2, 132.0, 137.4, 151.4, 157.3, 163.8; HRMS (ESI) calcd for [M + H]⁺ C₂₁H₁₈NO₂⁺: 316.13321 found 316.13113.

2.1.1.4. 4-(4-Chlorophenyl)-5-(4-methoxynaphthalen-1-yl)isoxazole (5d). Brown oil, yield 74%. ¹H NMR (400 MHz, CDCl₃) δ (ppm): 4.04 (s, 3H), 6.83 (d, 1H, *J* = 8.0 Hz), 7.11 (d, 2H, *J* = 8.8 Hz), 7.17 (d, 2H, *J* = 8.8 Hz), 7.41–7.45 (m, 1H), 7.47–7.52 (m, 2H), 7.64 (d, 1H, *J* = 8.4 Hz), 8.33

(d, 1H, *J* = 8.0 Hz), 8.60 (s, 1H); ¹³C NMR (100 MHz, CDCl₃) δ (ppm): 55.8, 103.5, 117.0, 117.1, 122.6, 125.0, 125.8, 126.0, 127.9, 128.3, 128.6, 129.1, 129.6, 132.0, 133.4, 150.3, 157.7, 165.3; HRMS (ESI) calcd for [M + H]⁺ C₂₀H₁₅ClNO₂⁺: 336.07858 found 336.07648.

2.1.1.5. 4-(2-Chlorophenyl)-5-(4-methoxynaphthalen-1-yl)isoxazole (5e). Yellow oil, yield 59%. ¹H NMR (400 MHz, CDCl₃) δ (ppm): 3.98 (s, 3H), 6.73 (d, 1H, *J* = 8.0 Hz), 6.99–7.00 (m, 2H), 7.14–7.18 (m, 1H), 7.38–7.49 (m, 4H), 7.82–7.84 (m, 1H), 8.28–8.30 (m, 1H), 8.63 (s, 1H); ¹³C NMR (100 MHz, CDCl₃) δ (ppm): 55.7, 103.3, 115.5, 117.0, 122.4, 125.1, 125.7, 125.8, 127.0, 127.6, 129.2, 129.4, 129.6, 130.1, 131.7, 132.0, 133.6, 151.9, 157.5, 166.7; HRMS (ESI) calcd for [M + H]⁺ C₂₀H₁₅ClNO₂⁺: 336.07858 found 336.07669.

2.1.1.6. 5-(4-Methoxynaphthalen-1-yl)-4-(2-methoxyphenyl)isoxazole (5f). Yellow oil, yield 65%. ¹H NMR (400 MHz, CDCl₃) δ (ppm): 3.65 (s, 3H), 4.00 (s, 3H), 6.69 (dt, 1H, *J* = 8.0 Hz, 0.8 Hz), 6.77 (d, 1H, *J* = 8.0 Hz), 6.86 (d, 1H, *J* = 8.4 Hz), 6.94 (dd, 1H, *J* = 8.0 Hz, 1.2 Hz), 7.18 (dt, 1H, *J* = 8.0 Hz, 1.6 Hz), 7.39–7.49 (m, 3H), 7.76 (d, 1H, *J* = 8.4 Hz), 8.30 (d, 1H, *J* = 8.0 Hz), 8.71 (s, 1H); ¹³C NMR (100 MHz, CDCl₃) δ (ppm): 55.3, 55.7, 103.3, 111.1, 114.3, 118.3, 118.8, 120.7, 122.3, 125.4, 125.7, 127.4, 129.2, 130.3, 132.2, 152.3, 156.7, 157.2, 165.5; HRMS (ESI) calcd for [M + H]⁺ C₂₁H₁₈NO₃⁺: 332.12812 found 332.12589.

2.1.1.7. 4-(3-Fluoro-4-methoxyphenyl)-5-(4-methoxynaphthalen-1-yl)isoxazole (5g). Yellow oil, yield 77%. ¹H NMR (400 MHz, CDCl₃) δ (ppm): 3.79 (s, 3H), 4.03 (s, 3H), 6.75 (t, 1H, *J* = 8.8 Hz), 6.83 (d, 1H, *J* = 8.8 Hz), 6.90–6.94 (m, 2H), 7.40–7.45 (m, 1H), 7.47–7.50 (m, 2H), 7.63 (d, 1H, *J* = 8.8 Hz), 8.32 (d, 1H, *J* = 8.8 Hz), 8.58 (s, 1H); ¹³C NMR (100 MHz, CDCl₃) δ (ppm): 55.8, 56.2, 103.5, 113.6, 115.0 (d, 1C, *J* = 19.4 Hz), 116.8, 117.2, 122.6, 122.7 (d, 1C, *J* = 7.1 Hz), 123.3 (d, 1C, *J* = 3.3 Hz), 125.0, 125.8 (d, 1C, *J* = 11.5 Hz), 126.0, 127.8, 129.6, 132.0, 147.0 (d, 1C, *J* = 10.6 Hz), 150.3, 151.1 (d, 1C, *J* = 244 Hz), 157.6, 164.7; HRMS (ESI) calcd for [M + H]⁺ C₂₁H₁₇FNO₃⁺: 350.11870 found 350.11618.

2.1.1.8. 5-(4-Methoxynaphthalen-1-yl)-4-(3-methoxyphenyl)isoxazole (5h). Yellow oil, yield 72%. ¹H NMR (400 MHz, CDCl₃) δ (ppm): 3.52 (s, 3H), 4.05 (s, 3H), 6.72–6.74 (m, 2H), 6.80 (d, 1H, *J* = 8.0 Hz), 6.84 (d, 1H, *J* = 8.0 Hz), 7.10–7.14 (m, 1H), 7.43–7.50 (m, 2H), 7.51 (d, 1H, *J* = 8.0 Hz), 7.66 (d, 1H, *J* = 8.4 Hz), 8.32 (d, 1H, *J* = 8.0 Hz), 8.63 (s, 1H); ¹³C NMR (100 MHz, CDCl₃) δ (ppm): 55.1, 55.8, 103.4, 112.8, 113.2, 117.6, 117.8, 119.8, 122.5, 125.3, 125.8, 125.9, 127.7, 129.6, 129.9, 131.0, 132.1, 150.5, 157.5, 159.8, 165.1; HRMS (ESI) calcd for [M + H]⁺ C₂₁H₁₈NO₃⁺: 332.12812 found 332.12585.

2.1.1.9. 4-(3,4-Dimethoxyphenyl)-5-(4-methoxynaphthalen-1-yl)isoxazole (5i). Yellow solid, yield 63%. ¹H NMR (400 MHz, CDCl₃) δ (ppm): 3.36 (s, 3H), 3.81 (s, 3H), 4.04 (s, 3H), 6.58 (d, 1H, *J* = 2.0 Hz), 6.72 (d, 1H, *J* = 8.4 Hz), 6.84–6.87 (m, 2H), 7.40–7.44 (m, 1H), 7.46–7.50 (m, 1H), 7.53 (d, 1H, *J* = 8.0 Hz), 7.65 (d, 1H, *J* = 8.4 Hz), 8.31 (d, 1H, *J* = 8.0 Hz), 8.62 (s, 1H); ¹³C NMR (100 MHz, CDCl₃)

δ (ppm): 55.5, 55.8, 55.9, 103.4, 110.4, 111.3, 117.7, 117.8, 119.7, 122.3, 122.5, 125.4, 125.7, 125.9, 127.7, 129.6, 132.1, 148.4, 148.9, 150.3, 157.4, 164.2; HRMS (ESI) calcd for $[M + H]^+ C_{22}H_{20}NO_4^+$: 362.13868 found 362.13586.

2.1.1.10. *4-(4-Ethoxyphenyl)-5-(4-methoxynaphthalen-1-yl)isoxazole (5j)*. Yellow solid, yield 68%. 1H NMR (400 MHz, $CDCl_3$) δ (ppm): 1.36 (t, 3H, $J = 6.8$ Hz), 3.92 (q, 2H, $J = 6.8$ Hz), 4.05 (s, 3H), 6.71 (d, 2H, $J = 8.8$ Hz), 6.83 (d, 1H, $J = 8.0$ Hz), 7.10 (d, 2H, $J = 8.8$ Hz), 7.40–7.47 (m, 1H), 7.49 (d, 2H, $J = 8.0$ Hz), 7.67 (d, 1H, $J = 8.4$ Hz), 8.32 (d, 1H, $J = 8.4$ Hz), 8.58 (s, 1H); ^{13}C NMR (100 MHz, $CDCl_3$) δ (ppm): 14.9, 55.8, 63.5, 103.4, 114.8, 117.7, 117.7, 121.9, 122.4, 125.3, 125.8, 125.9, 127.6, 128.6, 128.6, 129.5, 132.1, 150.6, 150.6, 157.4, 158.3, 164.2; HRMS (ESI) calcd for $[M + H]^+ C_{22}H_{20}NO_3^+$: 346.14377 found 346.14105.

2.1.1.11. *5-(4-Methoxynaphthalen-1-yl)-4-(o-tolyl)isoxazole (5k)*. Yellow oil, yield 92%. 1H NMR (400 MHz, $CDCl_3$) δ (ppm): 2.04 (s, 3H), 3.98 (s, 3H), 6.70 (d, 1H, $J = 8.0$ Hz), 7.09–7.19 (m, 4H), 7.28 (d, 1H, $J = 8.0$ Hz), 7.46–7.51 (m, 2H), 7.94–7.96 (m, 1H), 8.28–8.30 (m, 1H), 8.43 (s, 1H); ^{13}C NMR (100 MHz, $CDCl_3$) δ (ppm): 20.4, 55.7, 103.3, 117.1, 117.5, 122.4, 125.3, 125.8, 125.8, 126.2, 127.6, 128.2, 129.3, 129.6, 130.5, 130.6, 131.9, 136.8, 152.1, 157.3, 166.2; HRMS (ESI) calcd for $[M + H]^+ C_{21}H_{18}NO_2^+$: 316.13321 found 316.13095.

2.1.1.12. *4-(2-Fluorophenyl)-5-(4-methoxynaphthalen-1-yl)isoxazole (5l)*. White solid, yield 73%. 1H NMR (400 MHz, $CDCl_3$) δ (ppm): 4.04 (s, 3H), 6.81 (d, 1H, $J = 8.0$ Hz), 6.83–6.87 (m, 1H), 6.96 (dt, 1H, $J = 8.0$ Hz, 2.0 Hz), 7.05–7.10 (m, 1H), 7.15–7.21 (m, 1H), 7.41–7.51 (m, 3H), 7.69 (d, 1H, $J = 8.4$ Hz), 8.31 (d, 1H, $J = 8.0$ Hz), 8.68 (d, 1H, $J = 2.4$ Hz); ^{13}C NMR (100 MHz, $CDCl_3$) δ (ppm): 55.8, 103.4, 112.0, 116.0 (d, 1C, $J = 21.6$ Hz), 117.3, 117.7 (d, 1C, $J = 14.1$ Hz), 122.5, 124.3 (d, 1C, $J = 3.5$ Hz), 125.1, 125.8, 125.9, 127.7, 129.4, 129.5, 130.1 (d, 1C, $J = 3.0$ Hz), 132.0, 151.4 (d, 1C, $J = 6.6$ Hz), 157.5, 158.6 (d, 1C, $J = 247$ Hz), 166.1; HRMS (ESI) calcd for $[M + H]^+ C_{20}H_{15}FNO_2^+$: 320.10813 found 320.10593.

2.1.1.13. *4-(Benzo[d][1,3]dioxol-5-yl)-5-(4-methoxynaphthalen-1-yl)isoxazole (5m)*. Yellow solid, yield 79%. 1H NMR (400 MHz, $CDCl_3$) δ (ppm): 4.05 (s, 3H), 5.88 (s, 2H), 6.63–6.67 (m, 2H), 6.71 (dd, 1H, $J = 8.0$ Hz, 2.0 Hz), 6.84 (d, 1H, $J = 8.0$ Hz), 7.42–7.51 (m, 3H), 7.65 (d, 1H, $J = 8.0$ Hz), 8.31 (d, 1H, $J = 8.0$ Hz), 8.55 (s, 1H); ^{13}C NMR (100 MHz, $CDCl_3$) δ (ppm): 55.8, 101.2, 103.5, 107.9, 108.8, 117.4, 117.7, 121.2, 122.5, 123.6, 125.2, 125.8, 127.7, 129.5, 129.6, 132.1, 147.0, 148.0, 150.6, 157.5, 164.5; HRMS (ESI) calcd for $[M + H]^+ C_{21}H_{16}NO_4^+$: 346.10738 found 346.10468.

2.1.1.14. *4-(4-Fluorophenyl)-5-(4-methoxynaphthalen-1-yl)isoxazole (5n)*. Yellow oil, yield 58%. 1H NMR (400 MHz, $CDCl_3$) δ (ppm): 4.05 (s, 3H), 6.83–6.91 (m, 3H), 7.15–7.16 (m, 2H), 7.42–7.52 (m, 3H), 7.64 (d, 1H, $J = 8.4$ Hz), 8.33 (d, 1H, $J = 8.0$ Hz), 8.60 (s, 1H); ^{13}C NMR (100 MHz,

$CDCl_3$) δ (ppm): 55.9, 103.4, 115.8 (d, 1C, $J = 21.6$ Hz), 117.1 (d, 1C, $J = 12.6$ Hz), 122.6, 125.1, 125.8, 125.9, 126.0, 127.8, 129.1, 129.1, 129.2, 129.6, 129.6, 132.0, 150.5 (d, 1C, $J = 7.0$ Hz), 157.6, 160.9 (d, 1C, $J = 246.2$ Hz), 165.0; HRMS (ESI) calcd for $[M + H]^+ C_{20}H_{15}FNO_2^+$: 320.10813 found 320.10580.

2.1.1.15. *4-(4-Methoxy-3-nitrophenyl)-5-(4-methoxynaphthalen-1-yl)isoxazole (5o)*. Yellow solid, yield 86%. 1H NMR (400 MHz, $CDCl_3$) δ (ppm): 3.87 (s, 3H), 4.06 (s, 3H), 6.85–6.87 (m, 2H), 7.23 (dd, 1H, $J = 8.8$ Hz, 2.4 Hz), 7.42–7.46 (m, 1H), 7.49–7.53 (m, 2H), 7.60 (d, 1H, $J = 8.0$ Hz), 7.78 (d, 1H, $J = 8.0$ Hz), 8.33 (d, 1H, $J = 8.0$ Hz), 8.62 (s, 1H); ^{13}C NMR (100 MHz, $CDCl_3$) δ (ppm): 55.9, 56.6, 103.4, 114.0, 115.6, 116.6, 122.5, 122.7, 124.3, 124.8, 125.9, 126.1, 128.0, 129.7, 131.8, 133.0, 139.6, 150.0, 152.2, 157.8, 165.5; HRMS (ESI) calcd for $[M + H]^+ C_{21}H_{17}N_2O_5^+$: 377.11320 found 377.11050.

2.1.1.16. *2-Methoxy-5-(5-(4-methoxynaphthalen-1-yl)isoxazol-4-yl)aniline (5p)*. Yellow solid, yield 45%. 1H NMR (400 MHz, $CDCl_3$) δ (ppm): 3.77 (s, 3H), 4.04 (s, 3H), 6.56–6.62 (m, 3H), 6.82 (d, 1H, $J = 8.0$ Hz), 7.41–7.51 (m, 3H), 7.69 (d, 1H, $J = 8.0$ Hz), 8.31 (d, 1H, $J = 8.0$ Hz), 8.53 (s, 1H); ^{13}C NMR (100 MHz, $CDCl_3$) δ (ppm): 55.5, 55.7, 103.5, 110.7, 113.9, 117.8, 118.0, 118.1, 122.4, 122.7, 125.4, 125.7, 125.9, 127.5, 129.4, 132.4, 136.4, 146.9, 150.6, 157.4, 164.1; HRMS (ESI) calcd for $[M + H]^+ C_{21}H_{19}N_2O_3^+$: 347.13902 found 347.13663.

2.1.1.17. *4-(2-Bromophenyl)-5-(4-methoxynaphthalen-1-yl)isoxazole (5q)*. Yellow oil, yield 88%. 1H NMR (400 MHz, $CDCl_3$) δ (ppm): 3.98 (s, 3H), 6.72 (d, 1H, $J = 8.4$ Hz), 6.98 (dd, 1H, $J = 8.0$ Hz, 2.4 Hz), 7.04–7.11 (m, 2H), 7.36 (d, 1H, $J = 8.0$ Hz), 7.43–7.49 (m, 2H), 7.60 (dd, 1H, $J = 8.0$ Hz, 2.4 Hz), 7.85–7.88 (m, 1H), 8.27–8.30 (m, 1H), 8.61 (s, 1H); ^{13}C NMR (100 MHz, $CDCl_3$) δ (ppm): 55.7, 103.3, 116.9, 117.1, 122.4, 123.9, 125.2, 125.7, 125.8, 127.6, 129.6, 131.2, 132.0, 132.0, 133.3, 151.9, 157.4, 166.6; HRMS (ESI) calcd for $[M + H]^+ C_{20}H_{15}BrNO_2^+$: 380.02807 found 380.02530.

2.1.1.18. *4-(4-Bromophenyl)-5-(4-methoxynaphthalen-1-yl)isoxazole (5r)*. Yellow solid, yield 86%. 1H NMR (400 MHz, $CDCl_3$) δ (ppm): 4.05 (s, 3H), 8.34 (d, 1H, $J = 8.0$ Hz), 7.06 (d, 2H, $J = 8.0$ Hz), 7.31 (d, 2H, $J = 8.0$ Hz), 7.42–7.53 (m, 3H), 7.64 (d, 1H, $J = 8.8$ Hz), 8.33 (d, 1H, $J = 8.4$ Hz), 8.60 (s, 1H); ^{13}C NMR (100 MHz, $CDCl_3$) δ (ppm): 55.8, 103.4, 117.0, 117.1, 121.6, 122.6, 125.0, 125.8, 126.0, 127.9, 128.8, 128.9, 129.6, 132.0, 132.1, 150.3, 157.7, 165.3; HRMS (ESI) calcd for $[M + H]^+ C_{20}H_{15}BrNO_2^+$: 380.02807 found 380.02505.

2.1.1.19. *4-(3-Chlorophenyl)-5-(4-methoxynaphthalen-1-yl)isoxazole (5s)*. Yellow oil, yield 62%. 1H NMR (400 MHz, $CDCl_3$) δ (ppm): 4.05 (s, 3H), 6.83 (d, 1H, $J = 8.0$ Hz), 7.00–7.02 (m, 1H), 7.09 (t, 1H, $J = 8.0$ Hz), 7.15–7.18 (m, 1H), 7.26 (t, 1H, $J = 2.0$ Hz), 7.42–7.53 (m, 3H), 7.64 (d, 1H, $J = 8.4$ Hz), 8.33 (d, 1H, $J = 8.4$ Hz), 8.61 (s, 1H); ^{13}C NMR (100 MHz, $CDCl_3$) δ (ppm): 55.8, 103.4, 116.8, 117.0,

122.6, 125.0, 125.6, 125.8, 126.0, 127.3, 127.7, 127.8, 129.7, 130.1, 131.7, 132.0, 134.7, 150.4, 157.7, 165.6; HRMS (ESI) calcd for $[M + H]^+$ $C_{20}H_{15}ClNO_2^+$: 336.07858 found 336.07626.

2.1.1.20. *4-(3-Fluorophenyl)-5-(4-methoxynaphthalen-1-yl)isoxazole (5t)*. Yellow solid, yield 72%. 1H NMR (400 MHz, $CDCl_3$) δ (ppm): 4.06 (s, 3H), 6.85 (d, 1H, $J = 8.4$ Hz), 6.89–6.92 (m, 2H), 6.97 (d, 1H, $J = 8.0$ Hz), 7.14–7.19 (m, 1H), 7.41–7.46 (m, 1H), 7.48–7.52 (m, 2H), 7.63 (d, 1H, $J = 8.4$ Hz), 8.33 (d, 1H, $J = 8.0$ Hz), 8.62 (s, 1H); ^{13}C NMR (100 MHz, $CDCl_3$) δ (ppm): 55.9, 103.5, 114.4, 117.0, 122.5, 123.0, 123.2, 125.0, 125.8, 126.0, 127.8, 129.7, 130.5, 131.9, 132.0, 150.3, 150.4, 157.7, 161.7 (d, 1C, $J = 244.5$ Hz), 165.6; HRMS (ESI) calcd for $[M + H]^+$ $C_{20}H_{15}FNO_2^+$: 320.10813 found 320.10583.

2.1.1.21. *4-(3-Iodo-4-methoxyphenyl)-5-(4-methoxynaphthalen-1-yl)isoxazole (5u)*. Yellow oil, yield 57%. 1H NMR (400 MHz, $CDCl_3$) δ (ppm): 3.78 (s, 3H), 4.05 (s, 3H), 6.55 (d, 1H, $J = 8.4$ Hz), 6.83 (d, 1H, $J = 8.0$ Hz), 7.00 (dd, 1H, $J = 8.8$ Hz, 2.0 Hz), 7.44–7.52 (m, 3H), 7.66 (d, 1H, $J = 8.4$ Hz), 7.28 (d, 1H, $J = 2.0$ Hz), 8.32 (d, 1H, $J = 8.4$ Hz), 8.57 (s, 1H); ^{13}C NMR (100 MHz, $CDCl_3$) δ (ppm): 55.8, 56.4, 86.2, 103.4, 110.9, 116.2, 117.2, 122.5, 124.2, 125.2, 125.8, 126.0, 127.8, 128.7, 129.6, 132.0, 138.2, 150.4, 157.5, 157.6, 164.7; HRMS (ESI) calcd for $[M + H]^+$ $C_{21}H_{17}INO_3^+$: 458.02476 found 458.02042.

2.2. MTT assay

Human breast cancer cells (MCF-7) were seeded in 96-well plates and incubated for 24 h. Then treated with DMSO, cisplatin, or this series of compounds at the different concentrations (0.3125, 0.625, 1.25, 2.5, 5.0, 10.0 and 20.0 μ M) for 48 h. MTT (tetrazolium dye [3-(4,5-dimethylthiazol-2-yl)-2,5-diphenyltetrazolium bromide]) was added to each well, and incubated with cells at 37 °C for 4 h. Then, the formazan crystals were dissolved in DMSO, and the absorbency at 570 nm were measured by the Spectramax M5 Microtiter Plate Luminometer (Molecular Devices, USA). The IC_{50} value were presented as mean \pm standard deviation.

2.3. Tubulin polymerization assay

Tubulin protein was purified from fresh pig brain three cycles of temperature-dependent assembly/disassembly according to Shelanski et al in 100 mM PIPES (pH 6.5), 1 mM $MgSO_4$, 2 mM EGTA, 1 mM GTP and 1 mM 2-mercaptoethanol (Shelanski et al., 1973). In the first cycle of polymerization, glycerol and phenylmethylsulfonyl fluoride were added to 4 M and 0.2 mM, respectively. Homogeneous tubulin was prepared from microtubule protein by phosphocellulose (P11) chromatography.

After mixed tubulin protein with different concentrations of compound in PEM buffer (100 mM PIPES, 1 mM $MgCl_2$, and 1 mM EGTA) containing 1 mM GTP and 5% glycerol at 37 °C, the fluorescence intensity was monitored at 340 nm using a SPECTRA MAX 190 (Molecular Device) spectrophotometer. The plateau absorbance values were used for calculations.

2.4. Cell cycle analysis

Human breast MCF-7 cancer cells were seeded into the 6-well plate and treated with compound 5j (2.0 μ M) or DMSO for 24 h. After incubation, the cells were washed twice on ice with PBS and fixed with 70% ethanol at 4 °C overnight. Finally, the cells were treated with RNase and stained with propidium iodide (PI). The samples were analyzed by flow cytometry (TASC240, USA).

2.5. Cell apoptosis assay

Human breast MCF-7 cancer cells were seeded into the 6-well plate and treated with compound 5j (2.0 μ M) or DMSO. Cells were collected, washed, and stained with AnnexinV-FITC and PI. Then the sample was analyzed via flow cytometry (TASC240, USA).

2.6. Molecular docking study

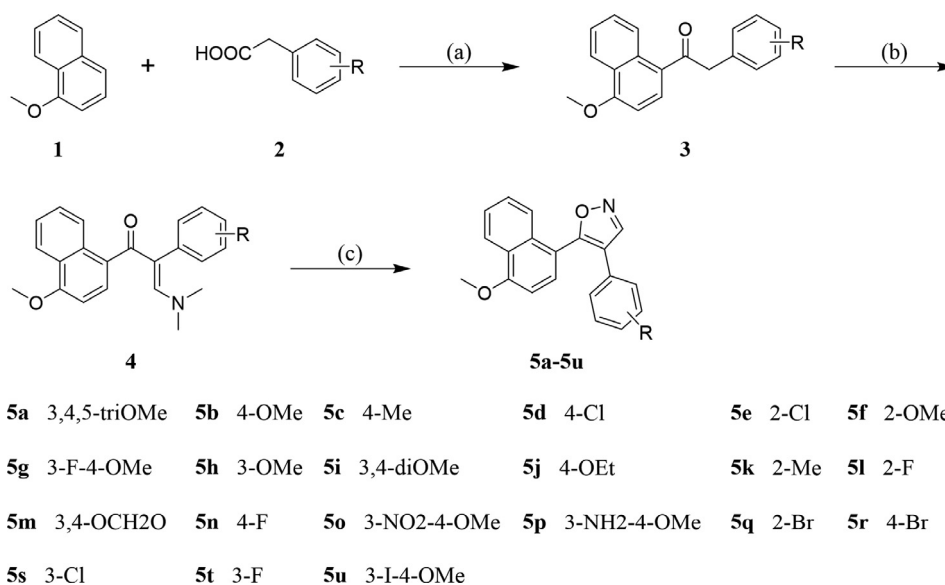
In this study, the tubulin structure (PDB ID: 1SA0) was downloaded from Protein Data Bank (www.rcsb.org). All bound waters and ligands were removed from the protein. The docking procedure was performed by using Autodock vina 1.1.2. The search grid of the tubulin was identified as center_x: 118.921, center_y: 89.718, and center_z: 5.932 with dimensions size_x: 15, size_y: 15, and size_z: 15. The value of exhaustiveness was set to 20. The best-scoring pose as judged by the Vina docking score was chosen and visually analyzed using PyMol 1.7.6 software (www.pymol.org).

3. Results and discussion

3.1. Chemistry

The synthetic pathway of the title compounds **5a-5u** was shown in Scheme 1. Condensation of 1-methoxynaphthalene **1** with various substituted phenylacetic acids **2** in the presence of trifluoroacetic acid (TFA) and trifluoroacetic anhydride (TFAA) to afford the corresponding deoxybenzoins **3** (Liu and Xu, 2018). Condensation of **3** with N,N-dimethylformamide dimethylacetal (DMF-DMA) to afford the enamines **4** in high yields, which reacted with hydroxylamine hydrochloride to provide the title compounds **5a-5u**.

All the synthesized compounds **5a-5u** were characterized by 1H NMR, ^{13}C NMR and HRMS spectroscopy (Supplemental Material, Figs. S1–S63). The 1H NMR of compound **5a** showed a singlet at δ 8.63 ppm representing the CH proton of isoxazole. The aromatic protons of 3,4,5-trimethoxyphenyl have appeared as a singlet for two protons at δ 6.39 ppm. The remaining six aromatic signals were assigned to the naphthalene nucleus in the compound **5a**. Characteristic methoxy protons appeared as three singlets at δ 3.47, 3.77 and 4.05 ppm. In ^{13}C NMR spectrum of compound **5a** the methoxy carbons appeared at δ 55.9, 55.9, and 61.0 ppm. All the aromatic carbons resonate around δ 103.3–164.7 ppm. The HRMS of compound **5a** showed a molecular ion peak at m/z 392.14603 as $[M + H]^+$ which also supports the proposed structure of the compound. A similar pattern



Scheme 1 Reagents and conditions: Reagents and conditions: (a) TFAA, TFA, room temperature, 12 h; (b) DMF-DMA, 80 °C, 24 h; (c) HONH₂·HCl, Na₂CO₃, AcOH, MeOH/H₂O, 70 °C, 24 h.

was observed in ¹H NMR, ¹³C NMR and HRMS of all the title compounds.

3.2. *In vitro* antiproliferative activity against breast cancer cell line (MCF-7)

The synthesized compounds **5a-5u** were tested for their antiproliferative activity against the human MCF-7 breast cancer cell line by using the standard MTT assay. Cisplatin was used as positive control drug. The IC₅₀ values (concentration required to cause 50% inhibition of the viability of cancer cells) of test compounds **5a-5u** and the positive control cisplatin are shown in Table 1. According to the experimental data, the majority of the tested compounds (except **5e**, **5l**, **5n** and **5s**) showed low antiproliferative activity with IC₅₀ values less than 10.0 μM. Compound **5b** and **5j** displayed the most potent antiproliferative activity with IC₅₀ values of 1.27 ± 0.13 μM and 1.23 ± 0.16 μM, respectively.

According to the anti-proliferative activity evaluations of these compounds mentioned above, the preliminary structure-activity relationships (SAR) of this class of compounds can be summarized. The results suggested that electron-donating group (Me, OMe, and OEt) located at the 4-position of the phenyl ring resulted in the best activity (**5a-5c**, **5g**, **5i**, **5j**, **5m**, **5p** and **5u**). Shifting methoxyl or methyl group to the 2- or 3- position decreased the activity (**5f**, **5h** and **5k**). Furthermore, introduction of electron withdrawing group (F, Cl, Br and NO₂) into the phenyl ring results in a significant decrease the inhibitory activity (**5d**, **5e**, **5l**, **5n**, **5o**, **5q**, and **5r-5t**). In particular, the substituent group located at the 2-position of the phenyl ring resulted in a decrease of inhibitory activity (**5e**, **5k**, **5l** and **5q**). Among this series of synthesized compounds, **5j** (IC₅₀ = 1.23 ± 0.16 μM) with 4-ethoxy substitution at phenyl ring was found to be the most active compound. Additionally, **5b** (IC₅₀ = 1.27 ± 0.13 μM) containing 4-methoxyl substitution at the phenyl ring was found to be the second most active compound.

Table 1 The *in vitro* anticancer activities of compounds **5a-5u** against human MCF-7 breast cancer cell line.

| Compd | R | IC ₅₀ (μM) | Compd | R | IC ₅₀ (μM) |
|-----------|--------------|-----------------------|------------------|--------------------------|-----------------------|
| 5a | 3,4,5-TriOMe | 2.55 ± 0.18 | 5l | 2-F | > 10.0 |
| 5b | 4-OMe | 1.27 ± 0.13 | 5m | 3,4-OCH ₂ O | 3.15 ± 0.24 |
| 5c | 4-Me | 2.03 ± 0.22 | 5n | 4-F | > 10.0 |
| 5d | 4-Cl | 5.26 ± 0.37 | 5o | 3-NO ₂ -4-OMe | 5.02 ± 0.46 |
| 5e | 2-Cl | > 10.0 | 5p | 3-NH ₂ -4-OMe | 3.09 ± 0.18 |
| 5f | 2-OMe | 8.13 ± 0.43 | 5q | 2-Br | 7.65 ± 0.36 |
| 5g | 3-F-4-OMe | 2.01 ± 0.22 | 5r | 4-Br | 4.41 ± 0.21 |
| 5h | 3-OMe | 3.51 ± 0.28 | 5s | 3-Cl | > 10.0 |
| 5i | 3,4-diOMe | 2.56 ± 0.15 | 5t | 3-F | 7.24 ± 0.37 |
| 5j | 4-OEt | 1.23 ± 0.16 | 5u | 3-I-4-OMe | 2.72 ± 0.14 |
| 5k | 2-Me | 7.61 ± 0.39 | Cisplatin | | 15.24 ± 1.27 |

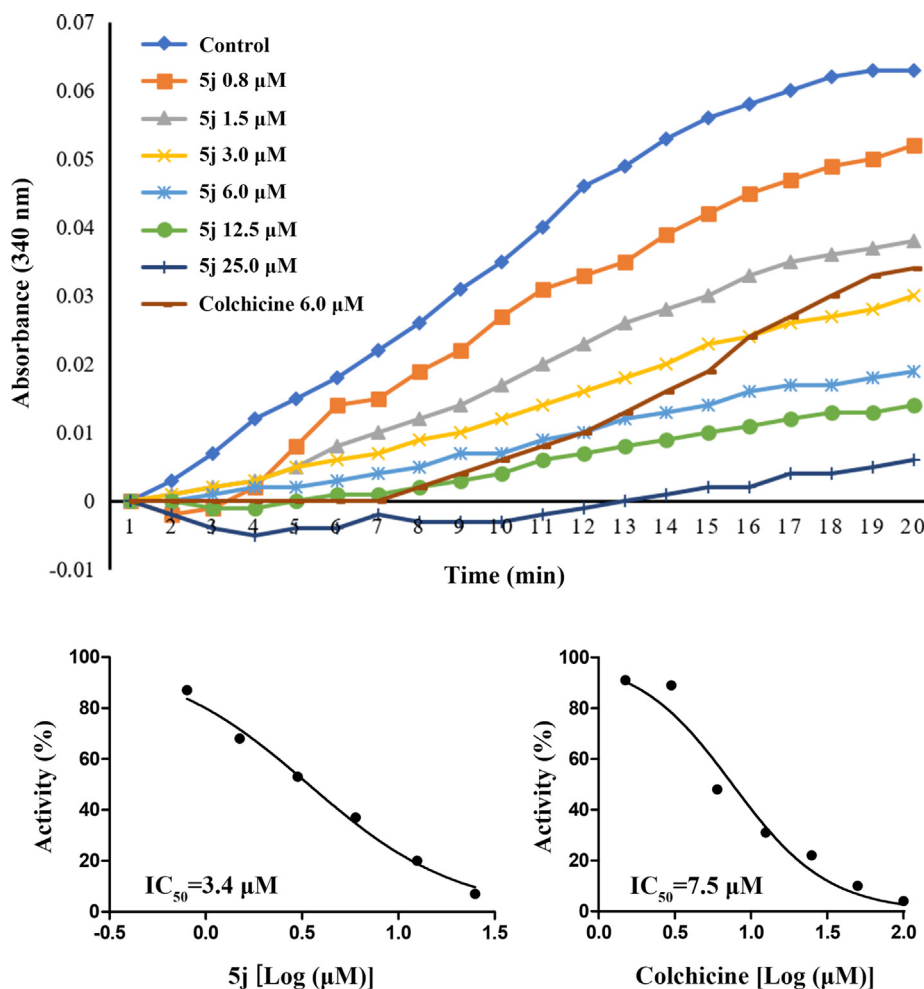


Fig. 3 Effect of compound **5j** and colchicine on tubulin polymerization.

3.3. Effect on tubulin polymerization

To investigate whether the antiproliferative activities of this class of compounds derived from interaction with tubulin, the most potent active compound **5j** was selected and evaluated for its inhibition of tubulin polymerization. For comparison, colchicine was used as a positive control. The results of this assay were shown in Fig. 3. After incubated tubulin protein with various concentrations of compound **5j** (0.8–25 μM), the increased tendency of the fluorescence intensity was obviously slowed down as compared with the control, which showed a trend similar to the positive colchicine. In addition, compound **5j** showed better inhibition of tubulin polymerization (IC₅₀ = 3.4 μM) than colchicine (IC₅₀ = 7.5 μM). These data confirmed that tubulin might be the molecular target of this series of compounds.

3.4. Cell cycle arrest

Based on the literature report, tubulin inhibitors could inhibit the polymerization of tubulin and thus cause cell cycle arrest in the G₂/M phase (Jordan, 2002). To verify whether these newly synthesized compounds could prevent mitosis, the effects of compound **5j** on cell cycle progression were examined by flow cytometry. MCF-7 cells were treated with DMSO or **5j**

(2.0 μM) for 24 h, and the proportion of tested cells at different cell cycle phases was analyzed by flow cytometry. As illustrated in Fig. 4, there was an accumulation of 83.30% of cells in the G₂/M phase of the cell cycle observed in **5j** treatment group, in contrast to that of untreated control (9.54%). Therefore, these observations indicated that compound **5j** could block the cell in the G₂/M phase and affect the normal mitosis of the cell.

3.5. Cell apoptosis

To verify whether compound **5j** could induce apoptosis of cancer cells, the effect of compound **5j** on cell apoptosis in MCF-7 was evaluated by using Annexin V-FITC/PI assay. As shown in Fig. 4, the cells were incubated with compound **5j** at 2.0 μM for 24 h, the percentages of early and late apoptosis cells were 15.3% and 6.44%, respectively, being elevated from the control group. These results confirmed that compound **5j** could induce apoptosis of MCF-7 cells, similar to other tubulin polymerization inhibitors.

3.6. Molecular docking

To elucidate the binding mode and type of interactions with tubulin (PDB code 1SA0), molecular docking simulations of the most active compound **5j** in the colchicine site of tubulin

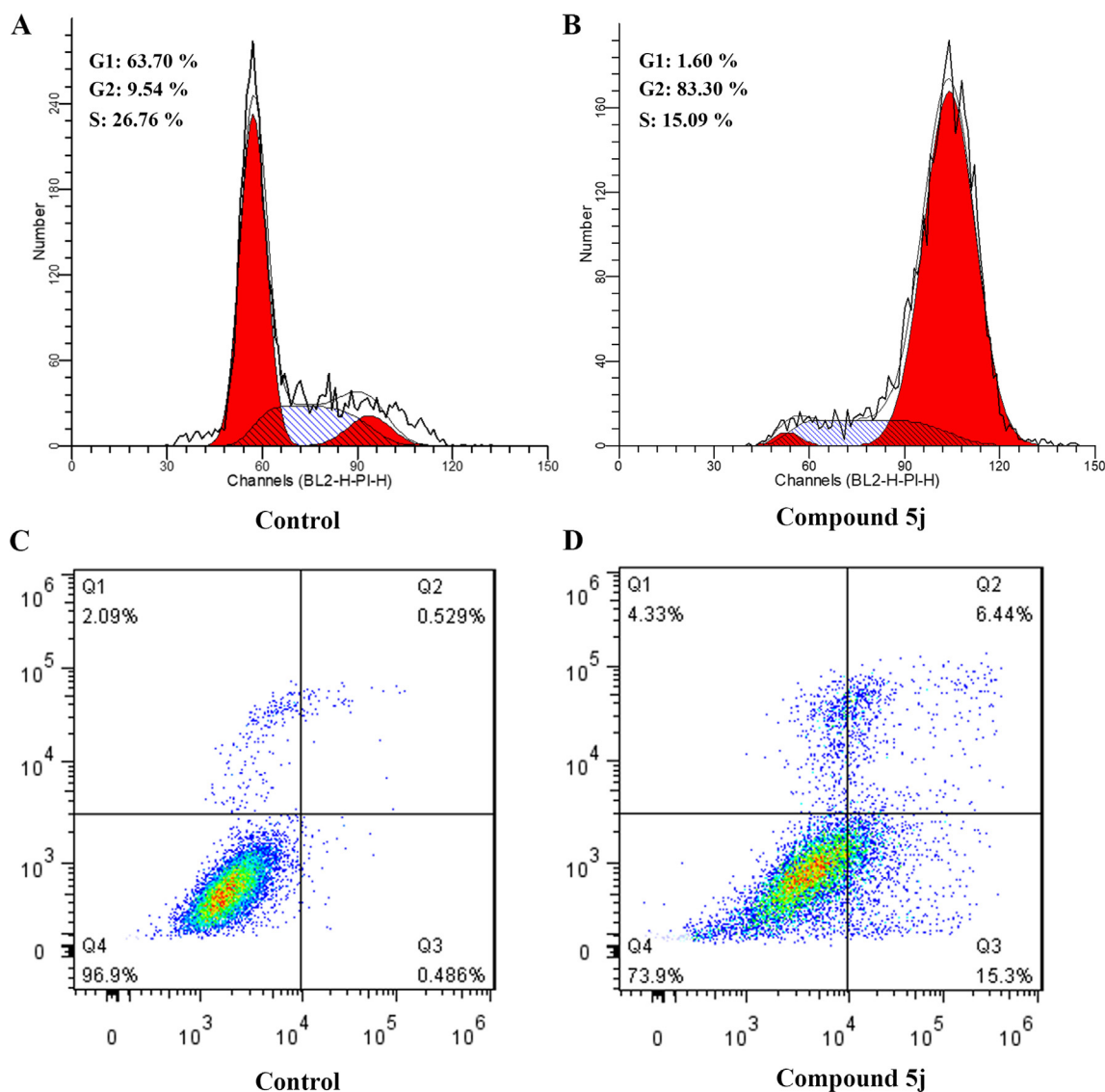


Fig. 4 Compound **5j** induced the cell cycle arrest and cell apoptosis in MCF-7 cells. (A, B) Cell cycle analysis of MCF-7 cells with or without treatment of **5j** for 24 h; (C, D) Cell apoptosis induction of MCF-7 cells with or without treatment of **5j** for 24 h.

were performed by using Autodock vina 1.1.2 (Trott and Olson, 2010). Colchicine was first docked into the colchicine binding site of tubulin. As shown in Fig. 5A, the docked conformation of colchicine is similar to the crystal conformation, indicating that this protocol of molecular docking is capable of reproducing the crystallographic pose. Then, we investigate the binding mode of compound **5j** with tubulin. The resulting binding mode is shown in Fig. 5B–D, Compound **5j** adopted an “L-shaped” conformation in the pocket of the tubulin. The estimated binding energy of compound **5j** with the enzyme was $-8.7 \text{ kcal}\cdot\text{mol}^{-1}$. The naphthyl group of **5j** located at the hydrophobic pocket, surrounded by the residues Cys-241, Leu-248, Ala-250, Leu-255, Met-259, Val-315, Ala-316, Val-318, and Ala-354, forming a strong hydrophobic binding. Detailed analysis showed that the phenyl group of **5j** formed cation- π interactions with the residues Lys-254 and Lys-352. Altogether, compound **5j** exhibited efficient binding to the colchicine site of tubulin, which provided a rational explanation of its inhibitory effect against tubulin.

4. Conclusion

In conclusion, a novel series of isoxazole-naphthalene derivatives (**5a–5u**) were synthesized and evaluated for their *in vitro* antiproliferative activity against human breast cancer cell line MCF-7. The antiproliferative assay indicated that the majority of the tested compounds (except **5e**, **5l**, **5n** and **5s**) displayed moderate to potent antiproliferative activity with IC_{50} values less than $10.0 \mu\text{M}$. Notably, compounds **5j** (4-ethoxy substitution) and **5b** (4-methoxy substitution) were found to be the most active compound in this series of compounds. Compound **5j** was over 10-fold more potent in inhibiting MCF-7 cell proliferation with IC_{50} values of $1.23 \pm 0.16 \mu\text{M}$ than the positive control drug cisplatin ($\text{IC}_{50} = 15.24 \pm 1.27 \mu\text{M}$). Flow cytometry analysis suggested that compound **5j** arrested cell cycle at G2/M phase and induces apoptosis in MCF-7 cell line. Moreover, *in vitro* polymerization assay was done and indicated that

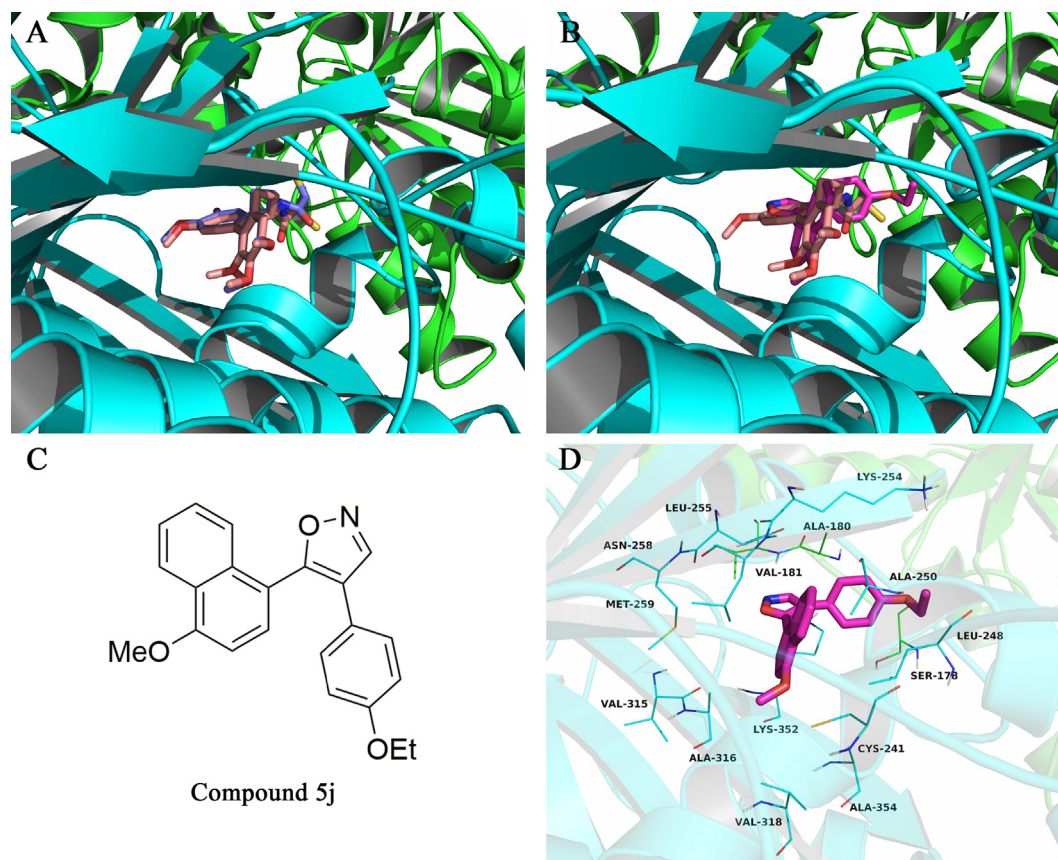


Fig. 5 (A) Redocked conformation superimposed on crystal conformation, the colchicine was shown in violet (docking conformation) or pink sticks (crystal conformation), respectively; (B) docked conformation of compound **5j** (rose red) superimposed on crystal conformation of the colchicine (pink); (c) Chemical Structure of compound **5j**; (d) Docking model of the most potent compound **5j** (magenta colour stick) in the colchicine binding site of tubulin.

compound **5j** more potently inhibited tubulin polymerization with IC_{50} value of $3.4 \mu\text{M}$ than positive control colchicine ($IC_{50} = 7.5 \mu\text{M}$). In silico molecular docking results showed that compound **5j** binds to the colchicine binding site of tubulin with good docking score $-8.7 \text{ kcal}\cdot\text{mol}^{-1}$. The results of our studies indicate that compound **5j** may be used as a novel lead compound in research on more effective anticancer agents by targeting the colchicine binding site of tubulin.

Declaration of Competing Interest

The authors declared that there is no conflict of interest.

Acknowledgments

This work was supported by National Natural Science Foundation of China (81660574), One Thousand Talents Program of Guizhou Province (the fifth group), Guizhou Provincial Natural Science Foundation ([2019]1256), Guizhou Province Administration of Traditional Chinese Medicine (QZYY-2019-057), the Doctor Foundation of Guizhou Medical University ([2018]004), the Science and Technology Fund of Guizhou Health Commission (gzwjkj2019-1-183), Guizhou Science and Technology Department ([2016]5613/5677, [2017] 5601), Local Science and Technology Project Guided by

Central Administration ([2018]4006), Guiyang Science and Technology Bureau ([2017]30-29).

Appendix A. Supplementary material

Supplementary data to this article can be found online at <https://doi.org/10.1016/j.arabjc.2020.04.014>.

References

- Alvarez, C., Alvarez, R., Corchete, P., Perez-Melero, C., Pelaez, R., Medarde, M., 2008. Naphthylphenstatins as tubulin ligands: Synthesis and biological evaluation. *Bioorg. Med. Chem.* 16 (19), 8999–9008. <https://doi.org/10.1016/j.bmc.2008.08.040>.
- Amos, L.A., 2011. What tubulin drugs tell us about microtubule structure and dynamics. *Semin. Cell Dev. Biol.* 22 (9), 916–926. <https://doi.org/10.1016/j.semedb.2011.09.014>.
- Badadhe, P.V., Patil, L.R., Bhagat, S.S., Chate, A.V., Shinde, D.W., Nikam, M.D., Gill, C.H., 2013. Synthesis and antimicrobial screening of some novel chromones and pyrazoles with incorporated isoxazole moieties. *J. Heterocycl. Chem.* 50 (5), 999–1004. <https://doi.org/10.1002/jhet.1545>.
- Caliskan, B., Sinoplu, E., Ibis, K., Guzelcan, E.A., Atalay, R.C., Banoglu, E., 2018. Synthesis and cellular bioactivities of novel isoxazole derivatives incorporating an arylpiperazine moiety as anticancer agents. *J. Enzyme Inhib. Med. Chem.* 33 (1), 1352–1361. <https://doi.org/10.1080/14756366.2018.1504041>.

- Colleoni, S., Jensen, A.A., Landucci, E., Fumagalli, E., Conti, P., Pinto, A., De Amici, M., Pellegrini-Giampietro, D.E., De Micheli, C., Mennini, T., Gobbi, M., 2008. Neuroprotective effects of the novel glutamate transporter inhibitor (-)-3-hydroxy-4,5,6,6a-tetrahydro-3aH-pyrrolo 3,4-d isoxazole-4-carboxylic acid, which preferentially inhibits reverse transport (glutamate release) compared with glutamate reuptake. *J. Pharmacol. Exp. Ther.* 326 (2), 646–656. <https://doi.org/10.1124/jpet.107.135251>.
- Desai, A., Mitchison, T.J., 1997. Microtubule polymerization dynamics. *Annu. Rev. Cell Dev. Biol.* 13, 83–117. <https://doi.org/10.1146/annurev.cellbio.13.1.83>.
- Downing, K.H., Nogales, E., 1998a. Tubulin and microtubule structure. *Curr. Opin. Cell Biol.* 10 (1), 16–22. [https://doi.org/10.1016/s0955-0674\(98\)80082-3](https://doi.org/10.1016/s0955-0674(98)80082-3).
- Downing, K.H., Nogales, E., 1998b. Tubulin structure: insights into microtubule properties and functions. *Curr. Opin. Struct. Biol.* 8 (6), 785–791. [https://doi.org/10.1016/s0959-440x\(98\)80099-7](https://doi.org/10.1016/s0959-440x(98)80099-7).
- Gomha, S.M., Badrey, M.G., Abdalla, M.M., Arafa, R.K., 2014. Novel anti-HIV-1 NNRTIs based on a pyrazolo 4,3-d isoxazole backbone scaffold: design, synthesis and insights into the molecular basis of action. *MedChemComm* 5 (11), 1685–1692. <https://doi.org/10.1039/c4md00282b>.
- Gorantla, V., Gundla, R., Jadav, S.S., Anugu, S.R., Chimakurthy, J., Rao, K.N.S., Korupolu, R., 2017. New anti-inflammatory hybrid N-Acyl hydrazone-linked isoxazole derivatives as COX-2 inhibitors: rational design, synthesis and biological evaluation. *ChemistrySelect* 2 (26), 8091–8100. <https://doi.org/10.1002/slct.201701421>.
- Hadfield, J.A., Ducki, S., Hirst, N., McGown, A.T., 2003. Tubulin and microtubules as targets for anticancer drugs. *Progr. Cell Cycle Res.* 5, 309–325.
- Jordan, A., Hadfield, J.A., Lawrence, N.J., McGown, A.T., 1998. Tubulin as a target for anticancer drugs: Agents which interact with the mitotic spindle. *Med. Res. Rev.* 18 (4), 259–296. [https://doi.org/10.1002/\(sici\)1098-1128\(199807\)18:4<259::Aid-med3>3.0.Co;2-u](https://doi.org/10.1002/(sici)1098-1128(199807)18:4<259::Aid-med3>3.0.Co;2-u).
- Jordan, M.A., 2002. Mechanism of action of antitumor drugs that interact with microtubules and tubulin. *Curr. Med. Chem. – Anti-Cancer Agents* 2 (1), 1–17. <https://doi.org/10.2174/1568011023354290>.
- Jordan, M.A., Wilson, L., 2004. Microtubules as a target for anticancer drugs. *Nat. Rev. Cancer* 4 (4), 253–265. <https://doi.org/10.1038/nrc1317>.
- Kaur, R., Kaur, G., Gill, R.K., Soni, R., Bariwal, J., 2014. Recent developments in tubulin polymerization inhibitors: An overview. *Eur. J. Med. Chem.* 87, 89–124. <https://doi.org/10.1016/j.ejmech.2014.09.051>.
- Koufaki, M., Fotopoulou, T., Kapetanou, M., Heropoulos, G.A., Gonos, E.S., Chondrogianni, N., 2014. Microwave-assisted synthesis of 3,5-disubstituted isoxazoles and evaluation of their anti-ageing activity. *Eur. J. Med. Chem.* 83, 508–515. <https://doi.org/10.1016/j.ejmech.2014.06.046>.
- Lee, S., Kim, J.N., Lee, H.K., Yoon, K.S., Shin, K.D., Kwon, B.-M., Han, D.C., 2011. Biological evaluation of KRIBB3 analogs as a microtubule polymerization inhibitor. *Bioorg. Med. Chem. Lett.* 21 (3), 977–979. <https://doi.org/10.1016/j.bmcl.2010.12.044>.
- Liu, G., Xu, B., 2018. Hydrogen bond donor solvents enabled metal and halogen-free Friedel-Crafts acylations with virtually no waste stream. *Tetrahedron Lett.* 59 (10), 869–872. <https://doi.org/10.1016/j.tetlet.2018.01.026>.
- Maya, A.B.S., Perez-Melero, C., Mateo, C., Alonso, D., Fernandez, J. L., Gajate, C., Mollinedo, F., Pelaez, R., Caballero, E., Medarde, M., 2005. Further naphthylcombretastatins. An investigation on the role of the naphthalene moiety. *J. Med. Chem.* 48 (2), 556–568. <https://doi.org/10.1021/jm0310737>.
- Medarde, M., Maya, A.B.S., Perez-Melero, C., 2004. Naphthalene combretastatin analogues: Synthesis, cytotoxicity and antitubulin activity. *J. Enzyme Inhib. Med. Chem.* 19 (6), 521–540. <https://doi.org/10.1080/14756360412331280473>.
- Messaoudi, S., Treguier, B., Hamze, A., Provot, O., Peyrat, J.-F., De Losada, J.R., Liu, J.-M., Bignon, J., Wdzieczak-Bakala, J., Thoret, S., Dubois, J., Brion, J.-D., Alami, M., 2009. Isocombretastatin A versus Combretastatin A: The forgotten isoCA-4 isomer as a highly promising cytotoxic and antitubulin agent. *J. Med. Chem.* 52 (14), 4538–4542. <https://doi.org/10.1021/jm900321u>.
- Santos, M.M.M., Faria, N., Iley, J., Coles, S.J., Hursthouse, M.B., Martins, M.L., Moreira, R., 2010. Reaction of naphthoquinones with substituted nitromethanes. Facile synthesis and antifungal activity of naphtho 2,3-d isoxazole-4,9-diones. *Bioorg. Med. Chem. Lett.* 20 (1), 193–195. <https://doi.org/10.1016/j.bmcl.2009.10.137>.
- Schwartz, E.L., 2009. Antivascular actions of microtubule-binding drugs. *Clin. Cancer Res.* 15 (8), 2594–2601. <https://doi.org/10.1158/1078-0432.ccr-08-2710>.
- Shelanski, M.L., Gaskin, F., Cantor, C.R., 1973. Microtubule assembly in the absence of added nucleotides. *PNAS* 70 (3), 765–768. <https://doi.org/10.1073/pnas.70.3.765>.
- Shin, K.D., Yoon, Y.J., Kang, Y.-R., Son, K.-H., Kim, H.M., Kwon, B.-M., Han, D.C., 2008. KRIBB3, a novel microtubule inhibitor, induces mitotic arrest and apoptosis in human cancer cells. *Biochem. Pharmacol.* 75 (2), 383–394. <https://doi.org/10.1016/j.bcp.2007.08.027>.
- Simoni, D., Grisolia, G., Giannini, G., Roberti, M., Rondanin, R., Piccagli, L., Baruchello, R., Rossi, M., Romagnoli, R., Invidiata, F.P., Grimaudo, S., Jung, M.K., Hamel, E., Gebbia, N., Crosta, L., Abbadessa, V., Di Cristina, A., Dusonchet, L., Meli, M., Tolomeo, M., 2005. Heterocyclic and phenyl double-bond-locked combretastatin analogues possessing potent apoptosis-inducing activity in HL60 and in MDR cell lines. *J. Med. Chem.* 48 (3), 723–736. <https://doi.org/10.1021/jm049622b>.
- Stanton, R.A., Gernert, K.M., Nettles, J.H., Aneja, R., 2011. Drugs that target dynamic microtubules: a new molecular perspective. *Med. Res. Rev.* 31 (3), 443–481. <https://doi.org/10.1002/med.20242>.
- Sysak, A., Obmińska-Mrukowicz, B., 2017. Isoxazole ring as a useful scaffold in a search for new therapeutic agents. *Eur. J. Med. Chem.* 137, 292–309. <https://doi.org/10.1016/j.ejmech.2017.06.002>.
- Trott, O., Olson, A.J., 2010. AutoDock Vina: improving the speed and accuracy of docking with a new scoring function, efficient optimization, and multithreading. *J. Comput. Chem.* 31 (2), 455–461. <https://doi.org/10.1002/jcc.21334>.
- Viegas-Junior, C., Danuello, A., Bolzani, V.D.S., Barreir, E.J., Manssour Fraga, C.A., 2007. Molecular hybridization: A useful tool in the design of new drug prototypes. *Curr. Med. Chem.* 14 (17), 1829–1852. <https://doi.org/10.2174/092986707781058805>.
- Wang, G., Wu, W., Peng, F., Cao, D., Yang, Z., Ma, L., Qiu, N., Ye, H., Han, X., Chen, J., Qiu, J., Sang, Y., Liang, X., Ran, Y., Peng, A., Wei, Y., Chen, L., 2012. Design, synthesis, and structure-activity relationship studies of novel millepachine derivatives as potent antiproliferative agents. *Eur. J. Med. Chem.* 54, 793–803. <https://doi.org/10.1016/j.ejmech.2012.06.034>.
- Wang, G., Li, C., He, L., Lei, K., Wang, F., Pu, Y., Yang, Z., Cao, D., Ma, L., Chen, J., Sang, Y., Liang, X., Xiang, M., Peng, A., Wei, Y., Chen, L., 2014. Design, synthesis and biological evaluation of a series of pyrano chalcone derivatives containing indole moiety as novel anti-tubulin agents. *Bioorg. Med. Chem.* 22 (7), 2060–2079. <https://doi.org/10.1016/j.bmc.2014.02.028>.
- Wang, G., Peng, Z., Zhang, J., Qiu, J., Xie, Z., Gong, Z., 2018a. Synthesis, biological evaluation and molecular docking studies of amino chalcone derivatives as potential anticancer agents by targeting tubulin colchicine binding site. *Bioorg. Chem.* 78, 332–340. <https://doi.org/10.1016/j.bioorg.2018.03.028>.
- Wang, G., Peng, Z., Peng, S., Qiu, J., Li, Y., Lan, Y., 2018b. (E)-N-Aryl-2-oxo-2-(3,4,5-trimethoxyphenyl)acetohydrazonoyl cyanides as tubulin polymerization inhibitors: Structure-based bioisosterism design, synthesis, biological evaluation, molecular docking and in silico ADME prediction. *Bioorg. Med. Chem. Lett.* 28 (20), 3350–3355. <https://doi.org/10.1016/j.bmcl.2018.09.004>.

- Wilson, L., Panda, D., Jordan, M.A., 1999. Modulation of microtubule dynamics by drugs: A paradigm for the actions of cellular regulators. *Cell Struct. Funct.* 24 (5), 329–335. <https://doi.org/10.1247/csf.24.329>.
- Wu, R., Ding, W., Liu, T., Zhu, H., Hu, Y., Yang, B., He, Q., 2009. XN05, a novel synthesized microtubule inhibitor, exhibits potent activity against human carcinoma cells in vitro. *Cancer Lett.* 285 (1), 13–22. <https://doi.org/10.1016/j.canlet.2009.04.042>.
- Yu, L., Tueckmantel, W., Eaton, J.B., Caldarone, B., Fedolak, A., Hanania, T., Brunner, D., Lukas, R.J., Kozikowski, A.P., 2012. Identification of novel alpha 4 beta 2-nicotinic acetylcholine receptor (nAChR) agonists based on an isoxazole ether scaffold that demonstrate antidepressant-like activity. *J. Med. Chem.* 55 (2), 812–823. <https://doi.org/10.1021/jm201301h>.
- Zhou, J., Giannakakou, P., 2005. Targeting microtubules for cancer chemotherapy. *Curr. Med. Chem. – Anti-Cancer Agents* 5 (1), 65–71. <https://doi.org/10.2174/1568011053352569>.
- Zhou, Z., Yan, J., Tang, X., Zhang, W., Zhang, Y., Chen, X., Su, X., Yang, D., 2010. Synthesis and preliminary evaluation of antidiabetic activity for beta-amino ketone containing isoxazole moiety. *Chin. J. Org. Chem.* 30 (4), 582–589.
- Zhu, J., Mo, J., Lin, H.-Z., Chen, Y., Sun, H.-P., 2018. The recent progress of isoxazole in medicinal chemistry. *Bioorg. Med. Chem.* 26 (12), 3065–3075. <https://doi.org/10.1016/j.bmc.2018.05.013>.